





This is to certify that the

thesis entitled

The Nigrorubral Projection and Rubrospinal Neurons in the Rat. Light and Electron Microscopic Studies utilizing a New Double-labeling Technique.

presented by

Kathy C. Bruce

has been accepted towards fulfillment of the requirements for

M.S. degree in Anatomy

Irena Grofowa, M.D., Ph.D.

Major professor

Date <u>4-22-92</u>

O-7639

MSU is an Affirmative Action/Equal Opportunity Institution

LIBRARY Michigan State University

PLACE IN RETURN BOX to remove this checkout from your record. TO AVOID FINES return on or before date due.

DATE DUE	DATE DUE	DATE DUE

MSU is An Affirmative Action/Equal Opportunity Institution c/circ/detectus.pm3-p.1

THE NIGRORUBRAL PROJECTION AND RUBROSPINAL NEURONS IN THE RAT. LIGHT AND ELECTRON MICROSCOPIC STUDIES UTILIZING A NEW DOUBLE-LABELING TECHNIQUE

By

Kathy C. Bruce

A THESIS

Submitted to
Michigan State University
in partial fulfillment of the requirements
for the degree of

MASTER OF SCIENCE

Department of Anatomy

ABSTRACT

THE NIGRORUBRAL PROJECTION AND RUBROSPINAL NEURONS IN THE RAT. LIGHT AND ELECTRON MICROSCOPIC STUDIES UTILIZING A NEW DOUBLE-LABELING TECHNIQUE.

By

Kathy C. Bruce

Projections of the substantia nigra pars reticulata (SNR) to red nucleus were studied light and electron microscopically using anterograde transport of *Phaseolus vulgaris* leucoagglutinin (PHA-L). The major purpose of the research was to test the hypothesis that the SNR input to the red nucleus may be distributed to rubrospinal neurons which are known to participate in the control of movement. To achieve this, we have developed a light and electron microscopic double-labeling technique combining PHA-L with the retrograde tracer Cholera toxin B (CTB). The results indicate that the nigrorubral fibers originate from ventral regions of the SNR, distribute throughout the rostrocaudal extent of the medial two-thirds of the red nucleus, and synapse preferentially with medium size dendrites. While many of the nigral varicose fibers were found apposing rubrospinal neurons, electron microscopic examination did not substantiate the existence of synaptic contacts between nigral boutons and rubrospinal neurons.

ACKNOWLEDGMENTS

I would like to thank my advisor, Dr. Irena Grofova, for her support, encouragement, and guidance not only during my graduate training but also while I worked as her research assistant. I have gained invaluable experience during those years. I would also like to thank Dr. Sharleen Sakai for her advice and support during my graduate training. I would like to acknowledge and thank the members of my graduate committee for their time and advice, Drs. Jim Hazlett, Duke Tanaka, and Sharleen Sakai. Thanks also to Deanna Wight for her assistance in the laboratory. And last but not least, thanks to my husband, Joe, for all his patience and support.

TABLE OF CONTENTS

LIST OF FIGURES v
ABBREVIATIONS viii
CHAPTER 1: NOTES ON A LIGHT AND ELECTRON MICROSCOPIC METHOD COMBINING ANTEROGRADE TRACING WITH PHA-L AND RETROGRADE TRACING WITH CTB
INTRODUCTION
MATERIALS AND METHODS PHA-L immunohistochemistry CTB immunohistochemistry PHA-L/CTB immunohistochemistry Electron microscopy: Single and sequential immunohistochemistry Controls
RESULTS
DISCUSSION 19
BIBLIOGRAPHY 22
CHAPTER 2: LIGHT AND ELECTRON MICROSCOPIC STUDIES ON THE ORGANIZATION OF THE NIGRORUBRAL CONNECTION IN THE RAT
INTRODUCTION
MATERIALS AND METHODS

RESULTS	31
Light Microscopic Observations	
Injections sites	31
Anterograde labeling of nigral fibers in the red nucleus	38
Coincidence of nigral terminal fields with CTB labeled	
rubrospinal neurons	39
Electron Microscopic Observations	
DISCUSSION	60
Technical considerations	60
Organization of the nigrorubral projection	63
Functional considerations	64
BIBLIOGRAPHY	66

LIST OF FIGURES

Chapter 1		
Figure 1:	Brightfield photomicrographs demonstrating anterograde transport of CTB and PHA-L.	12
Figure 2:	Brightfield photomicrographs demonstrating the results of combined PHA-L and CTB tract-tracing methods	14
Figure 3:	Electron micrographs depicting CTB labeled profiles	16
Figure 4:	Electron micrographs demonstrating the results of combined PHA-L and CTB tract-tracing methods	18
CHAPTER 2		
Figure 1:	Drawings of PHA-L deposits in the SNR	33
Figure 2:	Brightfield photomicrographs of PHA-L deposits in the SNR	35
Figure 3:	Brightfield photomicrographs of injection sites in double-labeling experiments	37
Figure 4:	Distribution of labeled nigral fibers in the red nucleus	41
Figure 5:	Brightfield photomicrographs of PHA-L immunoreacted sections from depicting the termination of nigral fibers in the red nucleus	43
Figure 6:	Brightfield photomicrograph illustrating nigral fibers in the red nucleus following a large PHA-L injection in the SNR	45
Figure 7:	Brightfield photomicrographs showing CTB labeled rubrospinal neurons (A) and the relationship of PHA-L labeled fibers to CTB labeled neurons (B)	47

Figure 8:	Electron micrographs of PHA-L labeled terminals in single-labeling case #12	51
Figure 9:	Electron micrograph of single-labeled material showing the relationship of a nigral terminal to a rubral neuron	53
Figure 10:	Low power electron micrograph of the double-labeled material	55
Figure 11:	Electron micrographs illustrating the relationship between a PHA-L labeled nerve terminal and a small CTB labeled cell body in the central portion of the red nucleus	57
Figure 12:	Electron micrograph showing a PHA-L labeled bouton in the neuropil adjacent to a large CTB labeled dendrite	59

ABBREVIATIONS

c caudal

CC central canal

cp cerebral peduncle

cu cuneate fasciculus

d dorsal

DpG deep gray layer of the superior colliculus

gr gracile fasciculus

HYP hypothalamus

ic internal capsule

IntG intermediate gray layer of the superior colliculus

lfu lateral funiculus spinal cord

ml medial lemniscus

MT medial terminal nucleus of the accessory optic tract

r rostral

R red nucleus

Rt reticular thalamic nucleus

SNC substantia nigra pars compacta

SNR substantia nigra pars reticulata

STH subthalamic nucleus

v ventral

vfu ventral funiculus spinal cord

VPL ventral posterolateral thalamic nucleus

VTA ventral tegmental nucleus

ZI zona incerta

CHAPTER 1

NOTES ON A LIGHT AND ELECTRON MICROSCOPIC METHOD COMBINING ANTEROGRADE TRACING WITH PHA-L AND RETROGRADE TRACING WITH CTB

INTRODUCTION

During the past two decades, there has been a significant increase in our knowledge of the anatomical and chemical organization of neuronal pathways. This is largely due to discoveries of sensitive anterograde and retrograde tracers and developments of immunohistochemical techniques. However, there is still need for improvement of double-labeling techniques that can be used at both light and electron microscopic levels and would allow determination of the synaptic arrangement of nerve terminals derived from a specific source with neurons projecting to anatomically defined targets. Anatomical evidence for monosynaptic pathways has been most frequently obtained from experiments utilizing retrograde transport of horseradish peroxidase conjugated to wheat germ agglutinin (HRP-WGA) in conjunction with degeneration of specific afferents following electrolytic or chemical lesions (Somogyi et. al., 1979; Tokuno and Nakamura, 1987; Williams and Faull, 1988; Nakamura et. al., 1989). This procedure has a number of limitations. First,

differences in the optimal survival time for the retrograde HRP labeling and maximal anterograde degeneration usually require a two-step surgery. Second, the degenerating terminals always exhibit different stages of degeneration. In an advanced stage, such terminals are often engulfed in glia and their normal morphology is obscured or severely distorted. On the other hand, early degenerative changes are difficult to differentiate from fixation artifacts. In the past years, an excellent anterograde tracing technique utilizing the transport and immunohistochemical visualization of the plant lectin Phaseolus vulgaris leucoagglutinin (PHA-L) became available (Gerfen and Sawchenko, 1984; Ter Horst et. al., 1984). This technique appears to be far superior to the degeneration method in tracing central neuronal connections at both light and electron microscopic levels (Wouterlood and Groenewegen, 1985). Unfortunately, the combination of anterograde PHA-L tracing with retrograde HRP labeling (Thompson and Thompson, 1988; Smith and Bolam, 1990) did not eliminate the need for two-step surgery. In addition the sensitivity of the two tracing techniques is compromised due to their differences in the optimal fixation. The strict fixation protocol required for PHA-L immunohistochemistry destroys enough of the enzymatic activity of the HRP to render the HRP labeled somata and proximal dendrites scarce and indistinct, particularly in the electron microscopic preparations (personal observations).

Recently, another sensitive tracer, unconjugated Cholera toxin subunit B (CTB), which is visualized by immunohistochemical methods has been successfully utilized in light and electron microscopic studies of nervous pathways in the central nervous system (Ericson and Blomqvist, 1988). The CTB is preferentially transported in the retrograde direction at a rate similar to that of PHA-L. Furthermore, the optimal fixation procedures are the same for CTB and PHA-L, and both tracers can be combined with neurotransmitter immunohistochemistry (Gerfen and Sawchenko, 1985; Wouterlood et. al., 1987; Smith and

Bolam, 1990) (PHA-L); (Fort et. al., 1989,1990; Rinaman and Miselis, 1990) (CTB).

In an attempt to determine possible input from the substantia nigra pars reticulata (SNR) to descending brainstem neurons, we have explored the combination of PHA-L as an anterograde tracer and unconjugated CTB as a retrograde tracer. In this report, we describe technical modifications that yielded the best quality light and electron microscopic double-labeled material.

MATERIALS AND METHODS

Twelve adult male albino rats (Sprague-Dawley) weighing between 250 and 350 grams were anesthetized with sodium pentobarbital (30 mg/kg, i.p.) and placed in a stereotaxic head holder (David Kopf). In single surgical sessions, single or multiple unilateral injections of PHA-L were made in SNR followed by bilateral injections of CTB in the cervical enlargement or medullary reticular formation. In cases in which CTB was injected in the cervical cord, animals were also fixed in a spinal unit (Kopf) and spinal laminectomies were performed. The stereotaxic coordinates were derived from the atlas of Paxinos and Watson (1986).

A 2.5% solution of PHA-L (Vector Labs) in 10 Mm Tris buffer (pH 8.0) was iontophoretically deposited for an interval of 20-30 minutes through a glass micropipette with an inside tip diameter of 10-30 μ m using a positive, 7s pulsed 5 μ A current (Midgard CS3 power source). Immediately following iontophoresis, pressure injections were made with CTB (Sigma or List Biological) which was reconstituted in distilled water to a final concentration of 1% (w/v) in a buffer of 0.5 M Tris containing 2 M NaCl, 0.03 M NaN₃, 0.01 M EDTA (pH 7.5). A Hamilton syringe fitted with a 25 gauge needle and a micropipette with an inside tip diameter of 50-60 μ m was used to deliver approximately 1

μl of CTB per site. After 4-10 days survival time, the animals were deeply anesthetized with sodium pentobarbital, heparinized, and perfused transcardially with a sodium phosphate buffered saline solution followed by 1 liter of fixative. For both light and electron microscopy one of the following fixatives were used: 1) 4% paraformaldehyde, 0.2% glutaraldehyde (EM grade) in 0.15M sodium phosphate buffer (pH 7.35) at 4° C (N = 6); or 2) PLP fixative (McLean and Nakane, 1974; Ericson and Blomqvist, 1988) containing 0.01 M sodium m-periodate (Sigma), 0.075 M D-L lysine (Sigma), and 3% paraformaldehyde in 0.01 M Sorenson's phosphate buffer (pH 6.0-7.4) at room temperature (N = 6). The brains and cervical cords were immediately removed and stored overnight at 4°C in fixative. Brains were divided into a left and right rostral block containing forebrain, midbrain, and rostral pons. Serial 50 µm thick sections from the rostral blocks were cut on a vibratome in the sagittal plane, collected in Tris buffered saline (TBS) at pH 7.63 and divided into three series of alternating sections (A, B, and C). Series A was processed for only PHA-L immunohistochemistry, series B was processed for only CTB immunohistochemistry, and series C was processed for PHA-L immunohistochemistry followed by CTB immunohistochemistry. Brainstem and cervical segments containing CTB deposits were cut in the transverse plane on a freezing microtome and processed for CTB immunohistochemistry along with series B. Selected sections from each series were further processed for electron microscopy.

PHA-L immunohistochemistry. The PHA-L immunohistochemistry was performed using a modified protocol by Gerfen and Sawchenko (1984). The sections were first rinsed in three changes of TBS containing 0.01%-0.04% Triton X-100 (optimal 0.02%)(TBS-TX) and then placed in a blocking solution of 3.0% normal rabbit serum in TBS. Following a 5 minute rinse, the sections were transferred to a 1:2000 dilution of primary goat anti-PHA-L

(Vector Labs) diluted in TBS-TX and incubated with gentle agitation for 48 hours at 4°C. The sections were then rinsed in TBS-TX and transferred to a 1:200 dilution of biotinylated rabbit anti-goat IgG (Vector Labs) in TBS-TX for 2 hours at room temperature with agitation. After additional rinses in TBS-TX, the sections were placed in a 1:1000 dilution of avidin-biotin-peroxidase complex (Vector Labs) in TBS-TX for 2 hours. The sections were rinsed and placed in a freshly prepared solution containing 100 mg 3,3'diaminobenzidine (DAB) (Sigma), 40 mg NH₄Cl, 200 mg B-D-glucose, and 0.4 mg glucose oxidase in 100 ml of 0.15 M Tris buffer for 15-25 minutes. After final rinses in Tris buffer, the sections for light microscopy were mounted onto gelatin-chromalum-coated slides, air-dried, dehydrated, and counter-stained with cresyl violet.

CTB immunohistochemistry. Sections for CTB immunohistochemistry were processed using the above described PHA-L protocol with the following modifications: 1) Following the blocking step in 3.0% normal rabbit serum and rinse, sections were placed in 1:100-1:5000 dilution of goat anti-choleragenoid (List Biological) diluted with TBS-TX and incubated with gentle agitation at 4°C for 60 hours; 2) Nickel chloride (final concentration 0.03%) was added to the DAB solution to produce a blue-black reaction product and the DAB reaction was carried for only 7-10 minutes. In some cases 0.03% nickel ammonium sulfate was added rather than nickel chloride. 3) Sections for light microscopy were mounted, air-dried, and cleared in xylene. Various counter-staining methods using cresyl-violet, neutral-red, or 0.01% osmium tetroxide were tested.

PHA-L/CTB immunohistochemistry. Protocols similar to the above were followed for the sequential double-labeling immunohistochemical reactions. Immediately after completion of the PHA-L reaction the sections were thoroughly rinsed in Tris buffer and placed directly

in 3.0% normal rabbit serum. Following the incubation in normal rabbit serum, the sections were treated according to the CTB immunohistochemical protocol. All solutions were used with the same dilutions and concentration of Triton X-100 as previously stated.

Electron microscopy: Single and sequential immunohistochemistry. Following the DAB reaction, selected sections were thoroughly washed in 0.15 M phosphate buffer (pH 7.35) and postfixed for 30 minutes in a 0.5% osmium tetroxide solution in 0.1 M phosphate buffer. The sections were dehydrated in graded acetone solutions and en bloc stained (3x 30% 10 min, 50% 10 min, 70% + 2% uranyl acetate 30 min, 95% 10 min, 2x 100% 10 min), infiltrated with Epon-Araldite, section embedded between a glass slide and coverslip coated with Liquid Release Agent, and polymerized (room temperature overnight, 40° 48 hrs, 60° 48 hrs, 80° 24 hrs).

Plastic embedded sections were first examined in the light microscope and areas exhibiting double-labeled profiles were documented on photomicrographs and/or projection drawings. The coverslip was then removed and a blank block was cemented on the selected region. The block was trimmed for ultrathin sectioning. Serial ultrathin sections (silver to pale gold interference color) were collected on formvar-coated slotted grids, stained with Reynold's lead citrate, and inspected in a JEOL-100CX electron microscope.

Controls. Brainstem and cervical sections containing only CTB deposits were incubated in PHA-L primary antisera to test for specificity and cross reactivity of the antibodies. After performing immunohistochemistry on such sections no reaction product was observed. Furthermore, the method specificity was ascertained by parallel single immunoreactions performed on adjacent sections (Series A: PHA-L only; series B: CTB only). Specific labeling patterns were obtained in each of these reactions.

RESULTS

Light microscopy. The PHA-L injection sites demonstrated a solid brown labeling of cells in the SNR. With the exception of a few solidly labeled cells along the pipette track, we have never observed any labeled cell bodies in the brainstem, diencephalon, striatum, or cerebral cortex. In several cases, the PHA-L was directly injected within the cerebral peduncle. Sections including such injections exhibited brown reaction product at the injection site, but there was no anterograde or retrograde labeling of fibers passing through this region. The CTB injections in the spinal cord or medullary reticular formation were generally small and often presented a tiny necrotic center surrounded by two zones of different labeling intensity as described by Ericson and Blomqvist (1988).

All experiments yielded very high contrast between the specific staining of immunopositive profiles and the unlabeled tissue. Sections processed for PHA-L immunohistochemistry (Series A) demonstrated a solid brown labeling of axons, their trajectories and terminal fields in the diencephalon and brainstem. Sections from Series B (CTB immunohistochemistry only) presented highly specific labeling of cells and fiber tracts. Neurons retrogradely labeled with CTB were characterized by the presence of blue-black granules in their cytoplasm while label was absent from the nucleus. The granules were large and often appeared fused due to the density of the label. The CTB reaction product extended into the primary as well as secondary dendrites. In general, the regional distribution of CTB labeled cells following multiple spinal cord injections was similar to that

previously described following HRP injections into the rat cervical cord (Leong et. al., 1984). However, it was observed that cells in some areas, particularly those containing large neurons, exhibited more intense labeling of the cell bodies and more complete filling of the dendrites. Such regions were consistent from case to case. Following both cervical cord and reticular formation injections, the CTB was also transported in the anterograde direction. In particular, the spinal cord injections always resulted in distinct labeling of the spinothalamic (Figure 1) and spinocerebellar fibers which could be followed to their terminal targets. In contrast to the solid appearance of the PHA-L label, the anterograde CTB reaction product exhibited punctate granules and the terminal and preterminal varicosities were somewhat more prominent than the fibers. Anterograde transport of CTB was always inferior in the intensity and completeness of labeling when compared to the anterograde transport of PHA-L and retrograde CTB labeling of cell bodies and dendrites.

In the double-labeled material (series C), the PHA-L labeled profiles could be clearly differentiated from the CTB labeled cells and fibers on the basis of the color differences (Figure 1B, 2). There was no decline in the intensity of either label nor was there an increase in background in sections submitted to sequential immunohistochemistry.

Electron microscopy. In ultrathin sections, the PHA-L reaction product was rather homogeneously distributed throughout the axoplasm of myelinated and unmyelinated fibers and nerve terminals (Figures 3, 4). The reaction product of retrogradely transported CTB was mainly associated with the Golgi apparatus in the cell bodies (Figures 3A; 4). It was also found in association with lysosomes in soma and large dendrites, and in smaller dendrites, with the membranes of mitochondria, multivesicular bodies, and neurotubuli (Figure 4). Anterogradely labeled CTB profiles were also readily recognized by electron microscopy. A fine punctate reaction product was found in axons and nerve terminals.

However, the reaction product was not homogeneously distributed and appeared to be concentrated in areas containing clusters of synaptic vesicles.

Technical comments. Injections made using CTB obtained from Sigma demonstrated superior transport, more intense labeling, and less background than those made using List CTB. A four day survival period was found to be optimal. In our hands, CTB labeling in cell bodies was less intense and dendritic label weak or absent when survival periods were greater than 4 days. Although there was no decline in the intensity of PHA-L label after 10 days survival, transport and anterograde label were not compromised with the shortened survival. The both tracers was suppressed by paraformaldehyde/glutaraldehyde fixation. PHA-L labeled profiles were visible but much less intense than those demonstrated in preparations with PLP fixation (compare Figures 2C, D). The CTB reaction product in cell bodies was weak and very granular and dendritic labeling, if present, was insubstantial in the presence of paraformaldehyde/glutaraldehyde fixative (Figure 2D). However, with PLP fixation, primary as well as secondary dendrites were clearly labeled (Figures 2C; 3). The reaction product in the neurons, though still granular, was far more dense. Ultrastructural preservation was adequate and the intensity of the electron dense reaction product of both tracers was augmented with PLP fixation.

Concentrations of Triton X-100 in the Tris buffered saline were varied from 0.01%-0.04%. Labeling with both PHA-L and CTB was optimal when 0.02% Triton X-100 was used. High background immunoreactivity of both tracers, but especially of CTB, was present when concentrations were decreased. At the electron microscopic level, we observed penetration of the antibodies throughout 50 μ m thick preparations with 0.02% Triton X-100. However, the reaction product of both tracers was weaker near the center of the sections. This concentration of Triton X-100 yielded the best compromise between ultrastructural

preservation and distinct labeling at both the light and electron microscopic levels.

Dilutions of goat-anti choleragenoid were varied between 1:100 and 1:5000. Concentration of 1:5000 yielded intense specific labeling of cell bodies with almost complete absence of background staining. As concentrations of the primary antibody increased, the amount of unspecific labeling also progressively increased.

Nickel chloride was found superior to nickel ammonium chloride for enhancement of the DAB reaction. Intense background staining over the entire section was present when nickel ammonium chloride was added to the DAB solution. Nickel chloride strongly enhanced the DAB reaction while producing a minimal amount of background staining. The pale gray staining of unlabeled neuronal cell bodies allowed recognition of cytoarchitectural boundaries (Figures 1, 2). In sections stored at room temperature without exposure to light, the NiCl₂-DAB reaction product has been stable over a period of one year with no decline in intensity. The CTB labeled profiles did exhibit a loss of intensity after counterstaining with cresyl violet or with neutral red. Dehydration during staining procedures was performed using graded alcohol or using graded acetone. However, both methods decreased the NiCl₂ enhancement of the CTB reaction product. Counterstaining with 0.01% OsO₄ gave relatively good results but, the color difference was less detectable. Since cytoarchitectural structures were definable with the NiCl₂ enhancement, omitting counterstaining entirely provided the best results.

Figure 1: Brightfield photomicrographs demonstrating anterograde transport of CTB and PHA-L.

- A: A double-labeled sagittal section through the lateral thalamus showing a sharply delineated area in the VPL containing anterogradely transported CTB. The PHA-L labeled nigral fibers are absent in this thalamic region. Pale gray staining of the non-labeled cells allows recognition of the nuclear boundaries. Fixative: PLP. Scale bar: 100 μm.
- B: Anterograde CTB labeling (block arrows) is intermingled with PHA-L labeled fibers in the intralaminar thalamic nuclei. Fixative: PLP. Scale bar: $50 \mu m$.

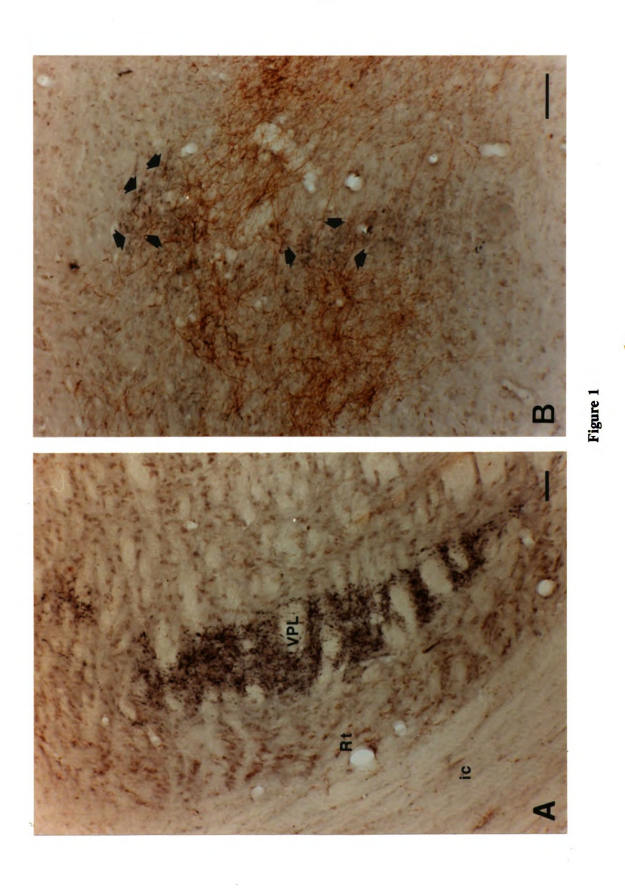


Figure 2: Brightfield photomicrographs demonstrating the results of combined PHA-L and CTB tract-tracing methods.

- A: Anterogradely PHA-L labeled nigral fibers (brown) form dense patches of terminal arborizations in the IntG and DpG layers of the superior colliculus.
 Large tectospinal neurons (blue-black) are prominent in the DpG. Fixative: PLP. Scale bar: 100 μm.
- B: High power photomicrograph of the area outlined in A showing the details of the PHA-L and CTB labeled profiles. Fixative: PLP. Scale bar: 50 μ m.
- C and D: Photomicrographs comparing the effect of different fixatives on retrograde CTB labeling and anterograde PHA-L labeling in the lateral hypothalamic area. The PLP fixative (C) enhanced both labels. In particular, the CTB reaction product is visible not only in the primary dendrites (solid arrow) but also in initial portions of the secondary dendritic branches (open arrows).

 D: 4% para formaldehyde, 0.02 % glutaraldehyde fixative. Scale bar: 50 μm.

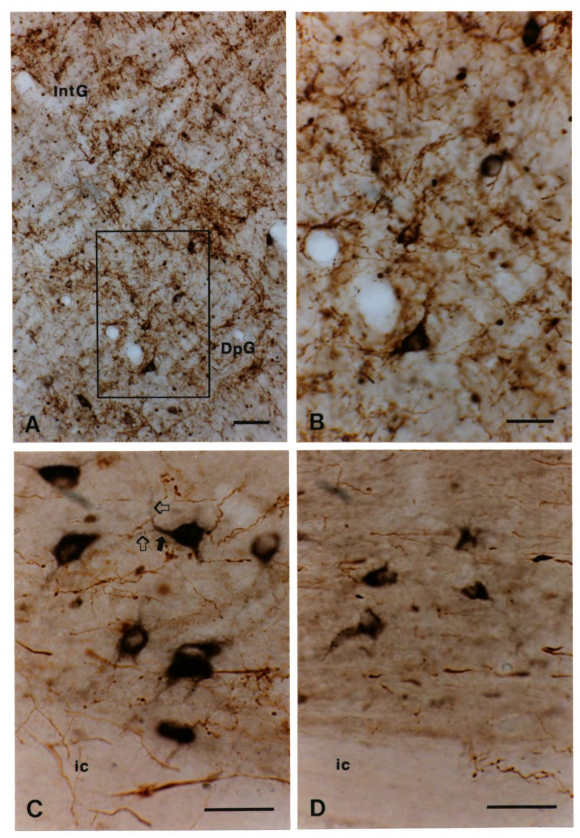


Figure 2

Figure 3: Electron micrographs depicting CTB labeled profiles.

- A: High power micrograph showing detail of the CTB reaction product associated with the Golgi apparatus (G) in a cell body. Cross-sectioned unlabeled dendrite (D1) and a CTB labeled dendrite (D2) are present in the lower portion of the picture. The reaction product within the dendrite enhances the outer mitochondrial membrane and neurotubuli. Scale bar: $1 \mu m$.
- B: Small CTB labeled dendrite (D) is contacted by two unlabeled boutons (B1 and B2). The CTB reaction product is again associated with the mitochondrial membrane, neurotubuli, and a structure (arrowhead) which is probably represents a multivesicular body. Scale bar: 500 nm.

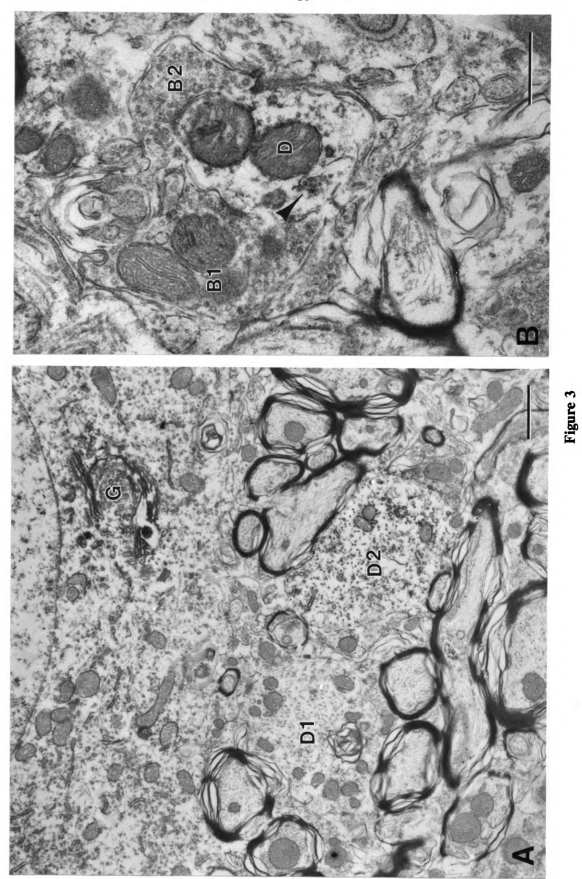


Figure 4: Electron micrographs demonstrating the results of combined PHA-L and CTB tract-tracing methods.

- A: Low power electron micrograph of a portion of a CTB labeled cell body and primary dendrite of a large rubrospinal neuron. The CTB reaction product is associated with the ruptured cisterns of the Golgi apparatus (arrows). Three PHA-L labeled myelinated fibers (open arrows) are found apposing the soma. Two PHA-L labeled unmyelinated fibers are seen in the surrounding neuropil (open arrows). Scale bar: 5 μm.
- B: High power electron micrograph of a PHA-L labeled nigral bouton (B) in synaptic contact (arrow) with a CTB labeled tectospinal neuron. The CTB reaction product in the cell body is indicated by arrowheads. Scale bar:
 1 μm.

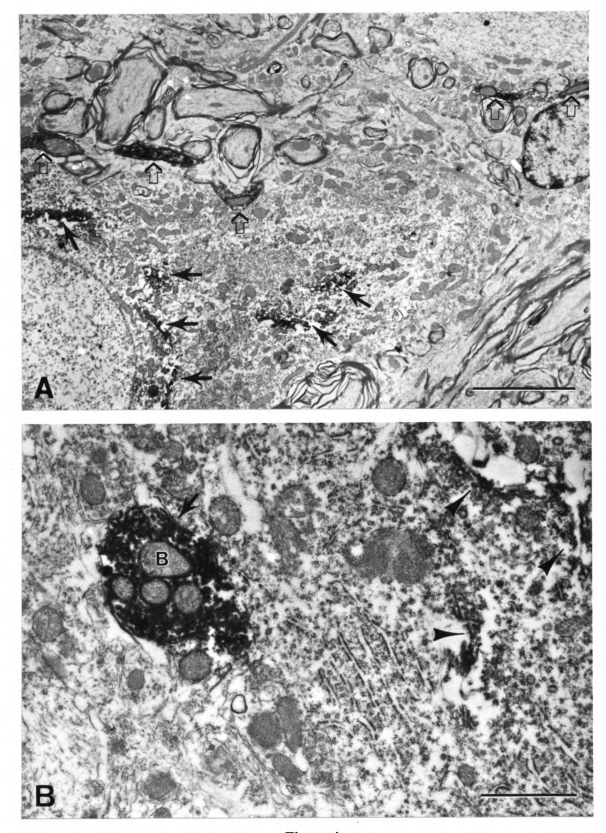


Figure 4

DISCUSSION

The present study demonstrates that the anterograde tracer PHA-L and the retrograde tracer unconjugated CTB can be used in conjunction for both light and electron microscopic studies of monosynaptic connections between specific afferents and CNS neurons projecting to a particular target. Both tracers have similar rates of transport which eliminates two-stage surgery, and they are fully compatible as to the optimal fixative. Using a sequential immunohistochemical protocol with nickel chloride added to the second DAB reaction, the double-labeled sections exhibit the PHA-L labeled and CTB labeled profiles in contrasting colors. This allows for easy and reliable recognition of congruent labels in the light microscope. It is only in the double-stained material that the precision of the correspondence between the specific afferent input and neurons projecting to a known region can be evaluated. While this objective can be achieved by combining the anterograde PHA-L tracing with retrograde transport of fluorescent dyes such as fast blue (Gerfen et. al., 1989), the presently described method is distinctly superior since it yields a permanent record. Even more important is the advantage that both labels can be readily recognized at the ultrastructural level. Therefore, the double-labeled material can also provide definitive evidence of monosynaptic contacts between identified afferents and projection neurons.

Each of the tracing techniques has its own benefits. The PHA-L method has been rather extensively used in different laboratories including our own, with excellent results.

The tracer and antibodies are commercially available and highly specific. The mechanisms of the PHA-L uptake and transport as well as its advantages over other anterograde markers have been previously discussed (Gerfen and Sawchenko, 1984; Ter Horst et. al., 1984; Gerfen and Sawchenko, 1985; Wouterlood and Groenewegen, 1985; Gerfen et. al., 1989). Briefly, the method provides Golgi-like labeling of the cells at the periphery of small injection sites and solid labeling of axons including their preterminal and terminal varicosities. There is generally almost complete absence of background immunoreactivity and relatively good staining of PHA-L labeled profiles in tissue preserved with glutaraldehyde and high concentrations of paraformaldehyde. However, the intensity of PHA-L staining appears much more prominent in material fixed with PLP fixative. The latter fixative also provides satisfactory preservation of the tissue for electron microscopy despite the complete absence of glutaraldehyde. In our hands, the tracer is not taken up and transported by damaged or undamaged axons passing through the injection site, as occasionally stated (Cliffer and Giesler, 1988; Schofield, 1989), and we have not observed any retrograde labeling following 4-10 days of survival.

The unconjugated CTB has been recently introduced as a retrograde tracer of central neuronal connections by Ericson and Blomqvist (1988). Using monoclonal antibodies raised in mouse hybridomas (Lindholm et. al., 1983), the authors (1988) have demonstrated that CTB is consistently transported in a number of central pathways, produces small injection sites, and impressive retrograde labeling involving not only cell bodies but also extensive portions of the dendritic trees. The extent and intensity of dendritic labeling in both light and electron microscopic preparations shown by Ericson and Blomqvist (1988) represent a major advantage of the CTB over HRP techniques, and is of particular importance for studies of the monosynaptic pathways since the dendrites commonly receive the majority of synaptic inputs. We have found that the dendritic labeling increases with short survival

times and critically depends on the type of fixative. The PLP fixative dramatically improved the extent and intensity of the labeled dendrites (compare Figures 2C, D).

Our results are consistent with the original observations (Ericson and Blomqvist, 1988) that CTB can be taken up and transported in both anterograde and retrograde directions by fibers of passage. The anterograde transport of CTB has been consistently present in our material, and was particularly prominent in cases involving substantial mechanical damage of the white matter at the injection site. In the context of the present double-labeling combination, the anterogradely transported PHA-L and CTB are very distinct in the light microscopic preparations due to the contrasting color. However, for ultrastructural examination of the nuclei containing both anterogradely and retrogradely transported CTB as well as anterogradely transported PHA-L, it would be necessary to use two chromogens yielding different types of electron dense reaction products, e.g. DAB for CTB and benzidine dihydrochloride (BDHC) or 3,3',5,5' tetramethylbenzidine (TMB) for PHA-L.

In conclusion, the combination of anterograde PHA-L and retrograde CTB tracing techniques represents a powerful tool for light and electron microscopic studies of monosynaptic pathways. Major advantages of this double-labeling technique over PHA-L\HRP or degeneration/HRP combinations include the compatibility of the two tracers with regard to the rate of transport and the optimal fixative. Additionally, the PHA-L/CTB technique can also be modified to study the organization of some superimposed afferent projections.

BIBLIOGRAPHY

- Cliffer, K.D. and G.J. Giesler, Jr. 1988. PHA-L can be transported anterogradely through fibers of passage. Brain Research 458:185-191.
- Ericson, H. and A. Blomqvist. 1988. Tracing of neuronal connections with cholera toxin subunit B: light and electron microscopic immunohistochemistry using monoclonal antibodies. J. Neurosci. Methods 24:225-235.
- Fort, P., K. Sakai, P.H.Luppi, D. Salvert, and M. Jouvet. 1989. Monoaminergic, peptidergic, and cholinergic afferents to the cat facial nucleus as evidenced by a double immunostaining method with unconjugated cholera toxin as a retrograde tracer. J. Comp. Neurol. 283:285-302.
- Fort, P., P.H. Luppi, K. Sakai, D. Salvert, and M. Jouvet. 1990. Nuclei of origin of monoaminergic, peptidergic, and cholinergic afferents to the cat trigeminal motor nucleus: A double-labeling study with Cholera-toxin as a retrograde tracer. J. Comp. Neurol. 301:262-275.
- Gerfen, C.R. and P.E. Sawchenko. 1984. An anterograde neuroanatomical tracing method that shows the detailed morphology of neurons, their axons and terminals: immunohistochemical localization of an axonally transported plant lectin, *Phaseolus vulgaris* leucoagglutinin (PHA-L). Brain Research 290:219-238.
- Gerfen, C.R. and P.E. Sawchenko. 1985. A method for anterograde axonal tracing of chemically specified circuits in the central nervous system: combined *Phaseolus vulgaris*-leucoagglutinin (PHA-L) tract tracing and immunohistochemistry. Brain Research 343:144-150.
- Gerfen, C.R., P.E. Sawchenko, and J. Carlsen. 1989. The PHA-L anterograde axonal tracing method. In L. Heimer and L. Záborszky (Eds.), Neuroanatomical Tract-Tracing Methods 2, Recent Progress, Plenum Press, New York, pp. 19-47.
- Leong, S.K., J.Y. Shieh, and W.C. Wong. 1984. Localizing spinal-cord-projecting neurons in adult albino rats. J. Comp. Neurol. 228:1-17.
- Lindholm, L., J. Holmgren, M. Wikström, U. Karlsson, K. Andersson, and N. Lycke. 1983. Monoclonal antibodies to cholera toxin with special reference to cross-reactions with *Escherichia coli* heat-labile enterotoxin. Infect. Immun. 40:570-576.

- McLean, I.W. and P.K. Nakane. 1974. Periodate-lysine-paraformaldehyde fixative a new fixative for immunoelectron microscopy. J. Histochem. Cytochem. 22:1077-1083.
- Nakamura, Y., H. Tokuno, T. Moriizumi, Y. Kitao, and M. Kudo. 1989. Monosynaptic nigral inputs to the pedunculopontine tegmental nucleus neurons which send their axons to the medial reticular formation in the medulla oblongata. An electron microscopic study in the cat. Neurosci. Lett. 103:145-150.
- Paxinos, G. and C. Watson. 1986. The Rat Brain in Stereotaxic Coordinates, 2nd edn., Academic Press, New York.
- Rinaman, L. and R.R. Miselis. 1990. Thyrotropin-releasing hormone-immunoreactive nerve terminals synapse on the dendrites of gastric vagal motoneurons in the rat. J. Comp. Neurol. 294:235-251.
- Schofield, R.P. 1989. Labeling of axons of passage by *Phaseolus vulgaris* leucoagglutinin (PHA-L). Neurosci. Abstr. 15:306.
- Smith, Y. and J.P. Bolam. 1990. The output neurones and the dopaminergic neurones of the substantia nigra receive a GABA-containing input from the globus pallidus in the rat. J. Comp. Neurol. 296:47-64.
- Somogyi, P., A.J. Hodgson, and A.D. Smith. 1979. An approach to tracing neuron networks in the cerebral cortex and basal ganglia. Combination of Golgi staining, retrograde transport of horseradish peroxidase and anterograde degeneration of synaptic boutons in the same material. Neuroscience 4:1805-1852.
- Ter Horst, G.J., H.J. Groenewegen, H. Karst, and P.G.M. Leiten. 1984. *Phaseolus vulgaris* leuco-agglutinin immunohistochemistry. A comparison between autoradiographic and lectin tracing of neuronal efferents. Trends Neurosci. 8:378-384.
- Thompson, A.M. and G.C. Thompson. 1988. Neural connections identified with PHA-L anterograde and HRP retrograde tract-tracing techniques. J. Neurosci. Methods 25:13-17.
- Tokuno, H. and Y. Nakamura. 1987. Organization of the nigrotectospinal pathway in the cat: a light and electron microscopic study. Brain Research 436:76-84.
- Williams, M.N. and R.L.M. Faull. 1988. The nigrotectal projection and tectospinal neurons in the rat. A light and electron microscopic study demonstrating a monosynaptic nigral input to identified tectospinal neurons. Neuroscience 25:533-562.
- Wouterlood, F.G. and H.J. Groenewegen. 1985. Neuroanatomical tracing by use of *Phaseolus vulgaris*-leucoagglutinin (PHA-L): electron microscopy of PHA-L filled neuronal somata, dendrites, axons and axon terminals. Brain Research 326:188-191.

Wouterlood, F.G., J.G.J.M. Bol, and H.W.M. Steinbusch. 1987. Double-label immunocytochemistry: Combination of anterograde neuroanatomical tracing with *Phaseolus vulgaris* leucoagglutinin and enzyme immunocytochemistry of target neurons. J. Histochem. Cytochem. 8:817-823.

CHAPTER 2

OF THE NIGRORUBRAL CONNECTION IN THE RAT

INTRODUCTION

The substantia nigra pars reticulata (SNR) and the internal segment of the globus pallidus (i.e. the entopeduncular nucleus in non-primates) represent major output stations of the basal ganglia system (Parent, 1986). This system consists of a group of interconnected subcortical nuclei including the caudate nucleus and putamen, globus pallidus, subthalamic nucleus, and the substantia nigra which play a critical role in the expression of normal movements. The SNR conveys the striatal and pallidal outflows to the thalamus, superior colliculus, and pedunculopontine tegmental nucleus (Beckstead et. al., 1979; Gerfen et. al., 1982; Spann and Grofova, 1991; Deniau and Chevalier, 1992). The main route in the control of somatic motor functions probably involves the nigro-thalamocortical circuit. In addition, the basal ganglia appear to control some aspects of motor behavior more directly through nigrotectal and nigropedunculopontine projections. The

nigrotectal projection has been implicated in the control of saccadic eye movements (Hikosaka and Wurtz, 1983; Hikosaka, 1989), and is known to control head and neck movements through a monosynaptic nigro-tecto-spinal pathway (Deniau and Chevalier, 1984; Williams and Faull, 1988). The nigropedunculopontine projection is also at least partially involved in motor functions (Garcia-Rill, 1986) by virtue of monosynaptic connections with the pedunculopontine neurons. These neurons send their axons to the major source of the reticulospinal tract, the medial reticular formation in the medulla (Garcia-Rill, 1986; Nakamura et. al., 1989). Nigral projections to other brainstem nuclei containing spinal cord projection neurons have not been documented. Among those structures, the red nucleus appears to be a particularly important source of fibers descending to the spinal cord and influences the activity of the spinal motor neurons.

Similar to other species, the red nucleus in the rat can be subdivided into a caudal, magnocellular portion consisting of giant (>40 μ m) and large neurons (26-40 μ m) and a rostral, parvocellular portion comprised of medium (20-25 μ m) and small neurons (<20 μ m) (Massion, 1967; Reid et. al., 1975). Although both the parvocellular and magnocellular divisions of the red nucleus project to the spinal cord, most spinal cord projecting neurons are located caudally (Flumerfelt, 1980; Reid, et. al., 1975; Shieh et. al., 1983). Within the magnocellular portion the rubrospinal neurons are somatotopically organized. Neurons located dorsally and dorsomedially project to the cervical cord and those located ventrally and ventrolaterally project to the lumbar cord (Flumerfelt and Gwyn, 1973; Shieh et. al., 1983; Strominger et. al., 1987). In addition, both divisions of the red nucleus send efferents to cerebellum as well as to the brainstem precerebellar nuclei, particularly the inferior olive and lateral reticular nucleus. Other rubral efferents distribute to the facial nucleus, trigeminal nuclei, vestibular complex, and the dorsal column nuclei (Flumerfelt and Hrycyshyn, 1985). The major afferents to the red nucleus arise from both the cerebral

cortex and cerebellum. The input from the motor cortex is limited to the parvocellular portion (Brown, 1974; Flumerfelt, 1980; Gwyn and Flumerfelt, 1974) whereas the afferents from the deep cerebellar nuclei distribute throughout the red nucleus in a topographical fashion. The interposed nucleus sends projections to the magnocellular red nucleus (Caughell and Flumerfelt, 1977; Daniel et. al., 1988; Dekker, 1981; Flumerfelt, 1980) while the parvocellular portion receives input from the dentate nucleus (Angaut and Cicirata, 1988; Caughell and Flumerfelt, 1977; Flumerfelt, 1980). The cerebellar inputs from the interposed and dentate nuclei influence the rubrospinal and rubro-olivary tracts, respectively (Caughell and Flumerfelt, 1977). The rubrospinal tract has an excitatory affect on alpha and gamma motorneurons which innervate flexor muscles, similar to that of the corticospinal tract (Kennedy, 1990; Massion, 1967, 1988). Therefore, we hypothesized that in addition to the nigrotectal and nigropedunculopontine projections the basal ganglia may also control motor behavior through a monosynaptic nigro-rubro-spinal pathway.

The purpose of the present study was two-fold. First to determine the existence of a connection linking the SNR to the red nucleus. Second, assuming the projection indeed exists, to establish whether or not the nigral fibers terminate on rubrospinal neurons. To label nigral efferents we utilized the anterograde tracer *Phaseolus vulgaris* leucoagglutinin (PHA-L), which is extremely sensitive and provides solid labeling of axons including the terminal arborizations and varicosities at both light and electron microscopic levels. This technique eliminates the limitations inherent to previously used autoradiographic and HRP methods, which cannot clearly differentiate between fibers passing through and terminating within a given region. An original double-labeling technique combining the anterograde transport of PHA-L with the retrograde transport of Cholera toxin subunit B (CTB) was employed at both light and electron microscopic levels to examine the possibility of monosynaptic contacts between the nigral fibers and rubrospinal neurons.

MATERIALS AND METHODS

A total of fifteen adult male albino rats (Sprague-Dawley) weighing between 250 and 350 grams were utilized for both the single- and double-labeling experiments. Eleven received multiple unilateral injections of PHA-L in the SNR while four were subjected to multiple unilateral PHA-L injections in the SNR followed by multiple bilateral injections of CTB in the cervical cord. For both surgeries and perfusions animals were deeply anesthetized with sodium pentobarbital (30 mg/kg, i.p.). Prior to surgery atropine sulfate solution (0.7 mg/kg, i.m.) was administered. Injections were made iontophoretically (PHA-L) or via a Hamilton syringe (CTB) using stereotaxic coordinates derived from the atlas of Paxinos and Watson (1986).

Single-labeling experiments. A 2.5% solution of PHA-L (Vector Labs) in 10 Mm Tris buffer (Ph 8.0) was iontophoretically deposited for an interval of 20-30 minutes through a glass micropipette with an inside tip diameter of 10-30 μ m using a positive, 7s pulsed 5 μ A current (Midgard CS3 power source). After 7-10 days survival time, the animals were deeply anesthetized and transcardially perfused with a sodium phosphate buffered saline solution followed by a fixative consisting of 4% paraformaldehyde and 0.2% glutaraldehyde (EM grade) in 0.15M sodium phosphate buffer. The brains were immediately removed and stored overnight at 4°C in fixative. Serial 30 μ m thick sections were cut on a vibratome in

the sagittal plane, collected in Tris buffered saline (TBS) and divided into two series of alternating sections. The first for light microscopic and the second for electron microscopic PHA-L immunohistochemistry using a modified protocol by Gerfen and Sawchenko ('84). The sections were first rinsed in three changes of TBS containing 0.2% Triton X-100 (TBS-TX) and then placed in a blocking solution of 3.0% normal rabbit serum in TBS. Following a 5 minute rinse, the sections were transferred to a 1:2000 dilution of primary goat anti-PHA-L (Vector Labs) diluted in TBS-TX and incubated with gentle agitation for 48 hours at 4°C. The sections were then rinsed in TBS-TX and transferred to a 1:200 dilution of biotinylated rabbit anti-goat IgG (Vector Labs) in TBS-TX for two hours at room temperature with agitation. After additional rinses in TBS-TX, the sections were placed in a 1:1000 dilution of avidin-biotin-peroxidase complex in TBS-TX for two hours. The sections were rinsed and placed in a freshly prepared solution containing 100 mg 3,3'diaminobenzidine (DAB) (Sigma), 40 mg NH₄Cl, 200 mg \(\beta\)-D-glucose, and 0.4 mg glucose oxidase in 100 ml of 0.15 M Tris buffer for 15-25 minutes. After final rinses in Tris buffer, the sections for light microscopy were mounted onto gelatin coated slides, air-dried, dehydrated, and counter-stained with cresyl violet. The sections were examined with a Leitz Orthoplan microscope using brightfield illumination. The localization of the PHA-L deposits in the SNR was charted on a map of sagittal sections passing through four equally spaced levels of the substantia nigra. The course and distribution of the labeled fibers in the red nucleus of selected immunoreacted sections were documented on projection drawings and/or photographed.

The series of sections selected for electron microscopy were processed using the same protocol with the concentration of Triton-X 100 in the TBS reduced to 0.04%. Following the DAB reaction selected sections were thoroughly washed in 0.15 M phosphate buffer and postfixed for 30 minutes in a 1% osmium tetroxide solution in 0.1 M phosphate

buffer. The sections were rinsed with dH₂O, en bloc stained with 2% uranyl acetate, and dehydrated in graded acetone solutions. Sections were then infiltrated with Epon-Araldite, section embedded between a glass slide and coverslip coated with Liquid Release Agent, and polymerized. Plastic embedded sections were first examined in the light microscope and areas exhibiting labeled profiles were documented on photomicrographs and/or projection drawings. The coverslip was then removed and a blank block was cemented on the selected region. The block was trimmed for ultrathin sectioning. Serial ultrathin (silver to pale gold interference color) sections were collected on formvar-coated slotted grids, stained with Reynold's lead citrate, and inspected in a JEOL-100CX electron microscope.

Double-labeling experiments. Surgical procedures for iontophoretic injections of PHA-L were not altered. Immediately following PHA-L iontophoresis a spinal laminectomy was performed and pressure injections were made with a 1% solution of CTB (Sigma) in distilled water. A Hamilton syringe fitted with a 25 gauge needle and a micropipette with an inside tip diameter of 30-50 μm was used to deliver approximately 1 μl of CTB per site. After 4-7 days survival, the animals were perfused as stated previously. However, a fixative consisting of 4% paraformaldehyde, 0.075 M lysine, and 0.01 M periodate in 0.01 M Sorenson's phosphate buffer (McLean and Nakane, 1974) was used rather than the paraformaldehyde/glutaraldehyde fixative. Serial 50 μm thick sections were vibratome cut in the sagittal plane and divided into three series of alternating sections (A, B, and C). Series A was processed for only PHA-L immunohistochemistry, series B was processed for only CTB immunohistochemistry, and series C was processed for PHA-L immunohistochemistry followed by CTB immunohistochemistry. Cholera toxin injection sites were coronally cut 50 μm thick on a freezing microtome and processed for CTB immunohistochemistry along with series B. A detailed description of the CTB and

sequential immunohistochemical protocols is provided in Chapter 1. Rubrospinal neurons were categorized by size based on cytoarchitectonic studies by Reid et. al. (1975).

RESULTS

Light Microscopic Observations

Injections sites. In the single-labeling experiments, the PHA-L deposits varied in size and involved different regions of the SNR. At the periphery of all PHA-L deposits, single SNR cells exhibited Golgi-like labeling and their axons could be traced towards the dorsal surface of the substantia nigra. Although in some cases small loci of PHA-L deposits were found in the cerebral peduncle, no labeled fibers were seen further caudally in the cerebral peduncle, pontine nuclei, or medullary pyramids. The pipette track was often visible as a discrete line of gliosis passing lateral to the red nucleus. Occasionally, a few PHA-L labeled cells were found along the track. Out of eleven single-labeling experiments, four (#12, #13, #14, and #15) showed consistently excellent anterograde labeling, precise localization of the injection in the substantia nigra, and a complete absence of labeled cells along the pipette track. In two of these cases (#12 and #15), the tracer was injected through three separate penetrations in order to label most of the SNR efferents. This procedure resulted in large PHA-L deposits which were most extensive medially involving the entire thickness of either the rostral two-thirds (#15) or caudal two-thirds (#12) of the SNR (Figures 1A; 2A, B). In contrast, single injections of PHA-L in cases #13 and #14 produced relatively small deposits limited to the ventral (#13) or dorsal (#14) portion of the midanteroposterior extent of the SNR (Figures 1A; 2 C, D). In the latter case, a few cells in the substantia

Figure 1: Drawings of PHA-L deposits in the SNR.

Drawings of sagittal sections through four lateromedial quarters of the SN (1: most lateral; 4: most medial) showing the extent of PHA-L deposits in the representative single-labeling (A) and double-labeling (B) experiments.

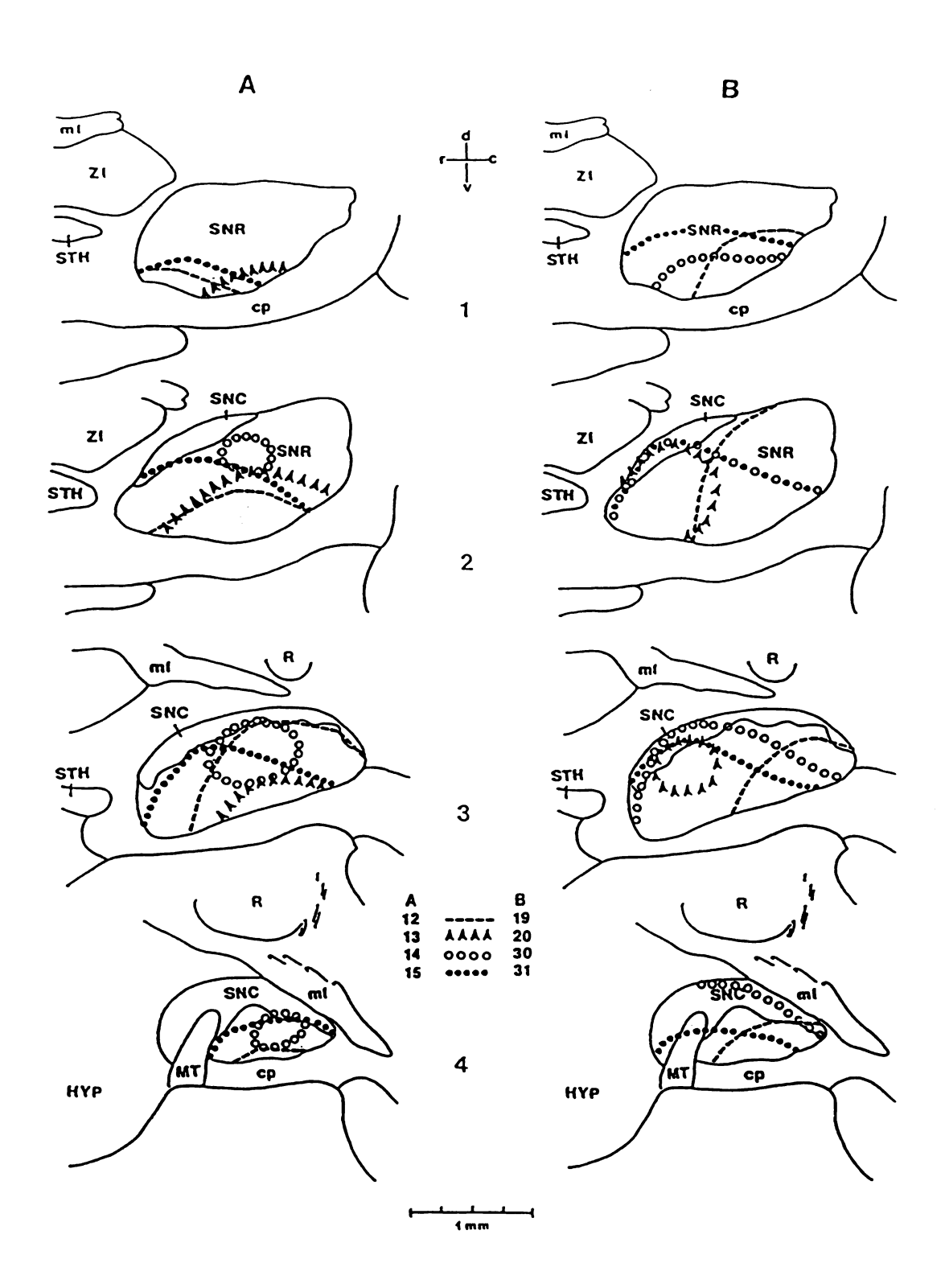


Figure 1

Figure 2: Brightfield photomicrographs of PHA-L deposits in the SNR.

Photomicrographs illustrating the central portion of the PHA-L deposits in the SNR in single-labeling cases #12 (A), #15 (B), #13 (C), and #14 (D). Note that the fibers of the cerebral peduncle do not contain the label. Scale bar: 0.5 mm.

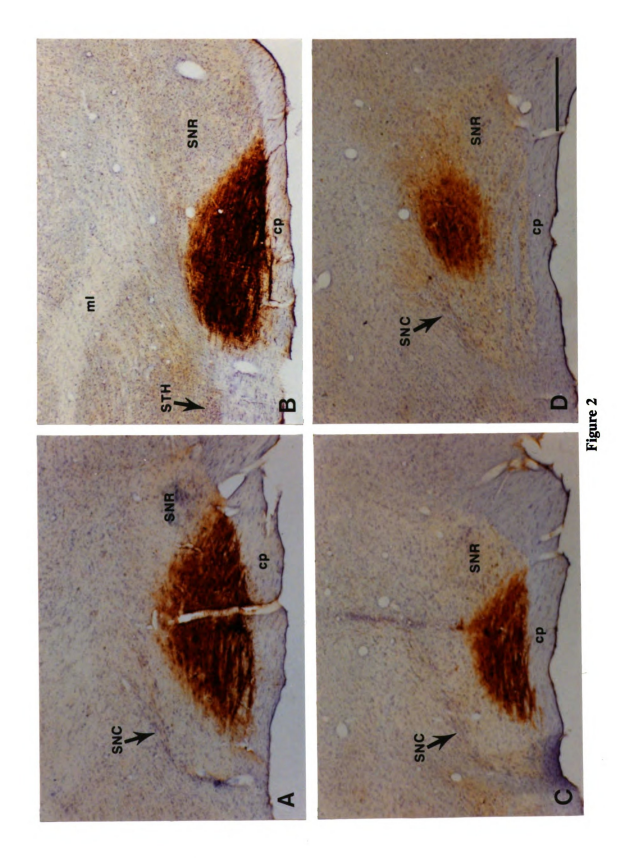


Figure 3: Brightfield photomicrographs of injection sites in double-labeling experiments.

- A: Photomicrograph illustrating the central portion of the PHA-L deposit in the SNR of case #20. Note again that the fibers of the cerebral peduncle are de void of label. Scale bar: 0.5 mm.
- B: Photomicrograph showing the localization of the CTB injections in the cervical cord of case #20. Asterisks denote the center of each deposit.Scale bar: 0.5 mm.

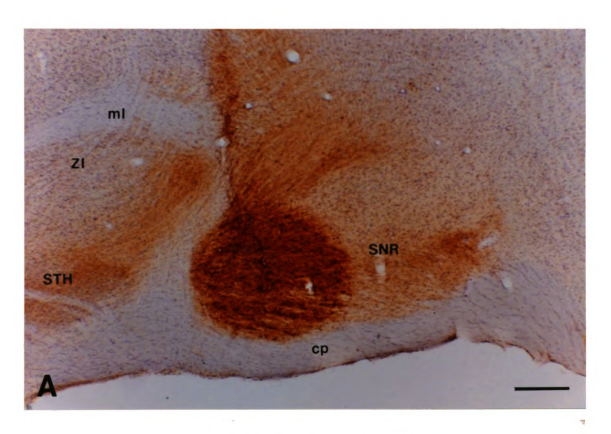




Figure 3

nigra pars compacta (SNC) were also labeled. In the remaining cases, the PHA-L deposits were smaller than in cases #12 and #15 and invariably involved ventral regions of the SNR.

Double-labeling experiments were conducted in four animals. In these cases (#19, #20, #30, and #31) both the PHA-L injections in the SNR and the CTB injections in the cervical cord were intentionally large in order to produce substantial anterograde labeling of the nigrorubral fibers and retrograde labeling of the rubrospinal neurons. The PHA-L was injected through two separate penetrations with pipette tracks passing lateral to the red nucleus. The extent of the PHA-L deposits in the SNR are illustrated in Figures 1B and 3A. No PHA-L labeled cells were observed in the tegmentum of the midbrain in any of these cases but the SNC invariably exhibited a modest number of labeled neurons. Multiple bilateral injections of the CTB in the cervical cord fused and spread throughout the gray matter and adjacent portions of the dorsolateral and ventral funiculi of the entire C3, C4, or C5 segments (Figure 3B). However, the location of each individual deposit could be recognized by the presence of a small necrotic center surrounded by a zone of intense labeling. The two centers of CTB injections frequently involved the ventrolateral aspect of the dorsal horn and intermediate region of the ventral horn, which represent the main regions of termination of the rubrospinal tract (Tracy, 1985). In several instances one of the CTB injections was centered in the dorsolateral funiculus through which passes the rubrospinal tract.

Anterograde labeling of nigral fibers in the red nucleus. The course of nigral fibers in the mesencephalic tegmentum and the distribution of fine terminal ramifications in the red nucleus in case #12 are illustrated in Figure 4. This distribution pattern was similar in all experiments except in case #14 in which the red nucleus was de void of labeled fibers.

Thick labeled fibers of even diameters exited the SN dorsally throughout its

mediolateral extent. Laterally, they pierced the medial lemniscus and entered the red nucleus via its ventral border. Fibers exiting the dorsomedial aspect of the SN collected in the pre-rubral field and entered the rostral pole of the red nucleus. In general, the lateral one-third of the red nucleus contained mainly thick fibers passing through the nucleus towards the tectum. In the more medial regions of the red nucleus, the labeled fibers ramified forming patches of terminal plexuses exhibiting numerous varicosities. The density of labeled varicose fibers was most prominent in the rostral parvocellular portion of the red nucleus and the varicosities were found in the neuropil as well as in close apposition to medium (20-25 μ m) and small (< 20 μ m) neurons (Figure 5). A smaller number of varicosities were also consistently seen in close proximity to large (26-40 μ m) and giant (> 40 μ m) neurons in the caudal magnocellular portion (Figure 6).

No anterograde transport of CTB was observed in the red nucleus, nor were any PHA-L labeled fibers seen in the contralateral red nucleus in any of the single- or double-labeling experiments.

Coincidence of nigral terminal fields with CTB labeled rubrospinal neurons. Retrogradely labeled rubrospinal neurons were observed throughout the extent of the red nucleus. However, the labeled cells were most numerous and the labeling most intense in its medial portion. The CTB reaction product was found in the soma of small, medium, large, and giant neurons as well as in primary and secondary dendrites. Nigral terminal fields were not only observed converging on groups of CTB labeled rubrospinal neurons, but also found in close association with non-labeled rubral cell bodies and other elements of the surrounding neuropil. Labeled nigral varicosities appeared to form perisomatic and peridendritic appositions to some of the retrogradely labeled rubrospinal neurons. Figure 7 shows the extent of retrograde labeling of the rubrospinal neurons and coincident PHA-L/CTB labels.

Figure 4: Distribution of labeled nigral fibers in the red nucleus.

Diagrammatic representation of the distribution of PHA-L lableld fibers in four lateromedial quarters (A: most lateral; D: most medial) of the ipsilateral red nucleus following a large PHA-L injection in the SNR (case #12).

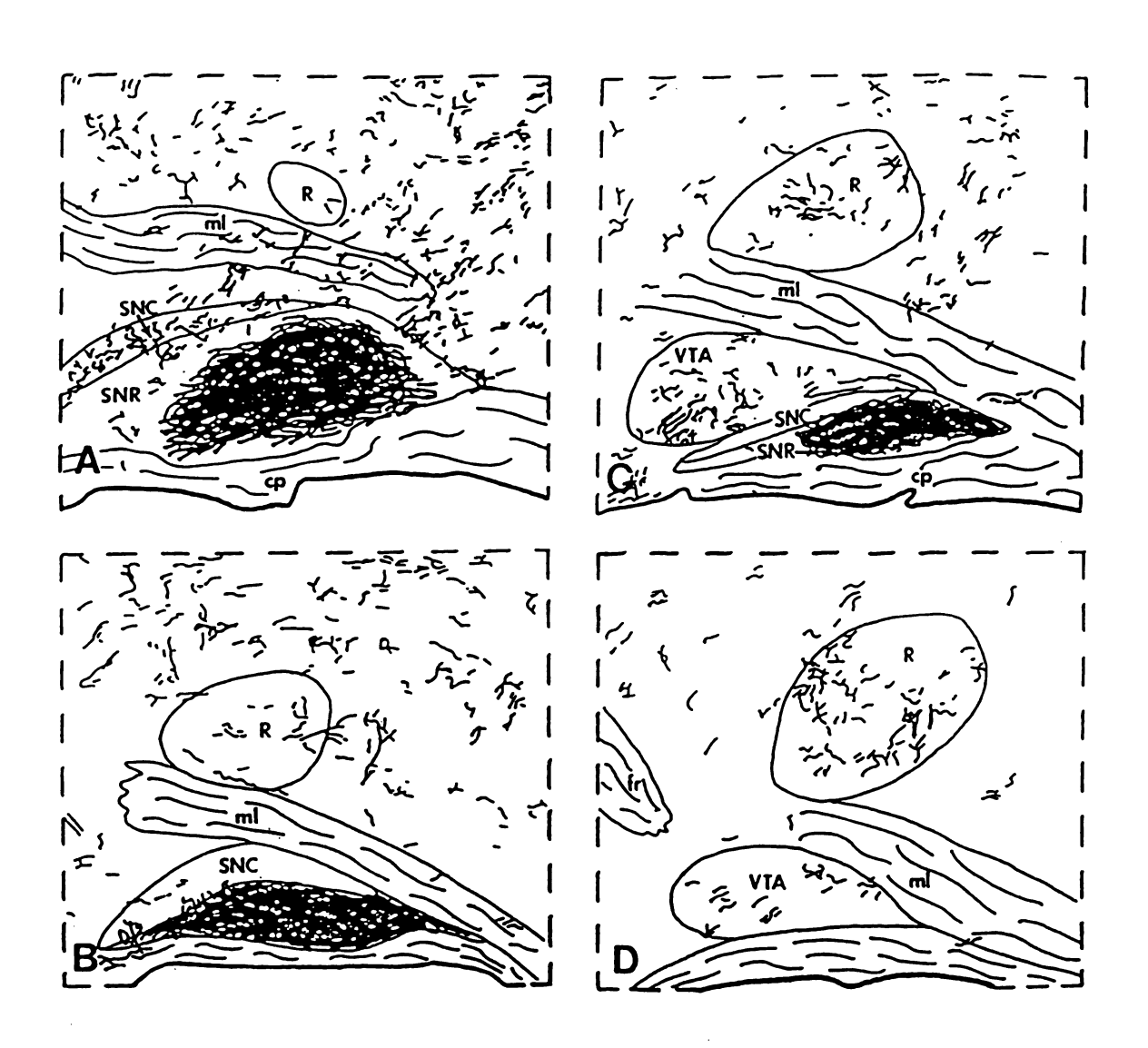


Figure 4

Figure 5: Brightfield photomicrographs of PHA-L immunoreacted sections from depicting the termination of nigral fibers in the red nucleus.

- A: Low power photomicrograph showing patches of nigral terminal plexuses in the rostral portion of red nucleus following a small PHA-L deposit in the ventral portion of the SNR (case #13). Scale bar: $100 \mu m$.
- B: High power photomicrograph of the area outlined in A illustrating the plexuses of labeled fibers with numerous varicosities. Many varicose fibers were in apposed to rubral neurons (arrows). Scale bar: $100 \mu m$.

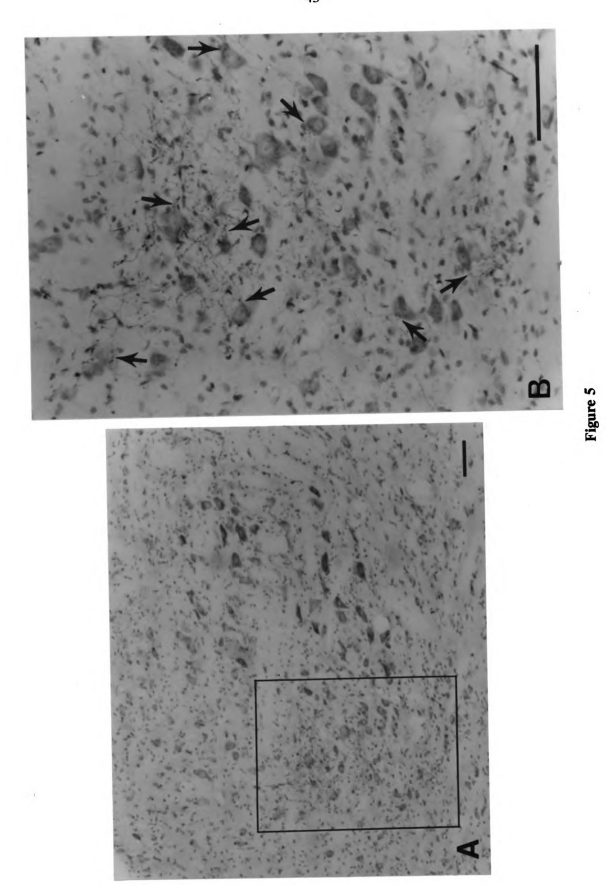


Figure 6: Brightfield photomicrograph illustrating nigral fibers in the red nucleus following a large PHA-L injection in the SNR.

High power photomicrograph showing PHA-L labeled fibers and varicosities in the caudal pole of the red nucleus in case #15. Arrows indicate the labeled fibers and swellings apposing large or giant rubral neurons. Scale bar: $100 \mu m$.

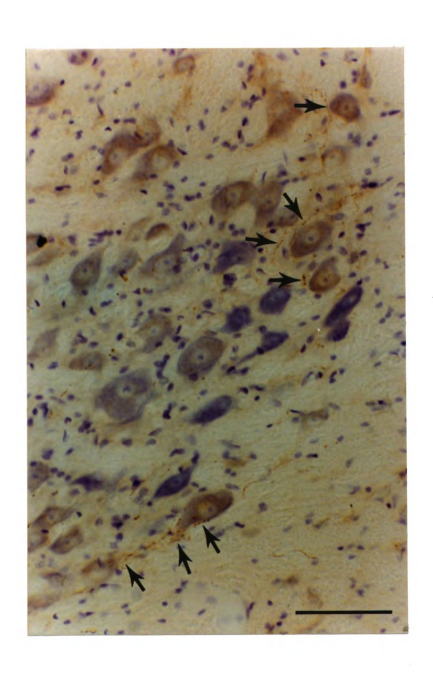


Figure 6

- Figure 7: Brightfield photomicrographs showing CTB labeled rubrospinal neurons (A) and the relationship of PHA-L labeled fibers to CTB labeled neurons (B).
 - A: Photomicrograph of a section reacted for CTB immunohistochemistry only demonstrating numerous labeled neurons in the caudal pole of the red nucleus. The reaction product is present in cell bodies of various sizes as well as in primary and secondary dendrites (arrows). Scale bar: $100 \mu m$.
 - B: Photomicrograph of a section submitted to double-immunohistochemistry illustrating a patch of PHA-L labeled terminal fibers (brown) congruent with a group of CTB labeled neurons (black). Arrows indicate nigral varicose fibers in close proximity to labeled rubrospinal neurons. Scale bar: $100 \mu m$.

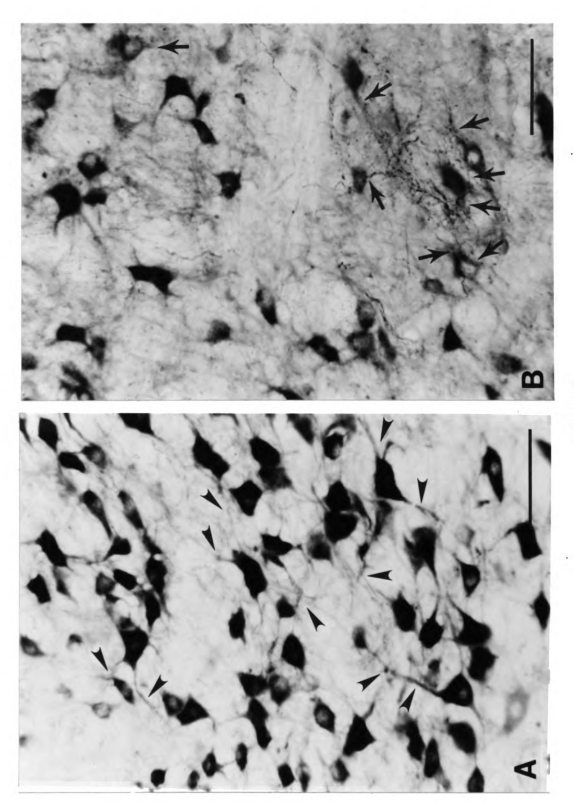


Figure 7

Electron Microscopic Observations

Postfixation with osmium tetroxide greatly enhanced the intensity of the DAB reaction product in both single- and double-labeled material. Although the color difference in the double-labeled tissue was lost after osmication, the labels could be easily identified. Regions exhibiting the densest PHA-L labeled plexuses (single-labeling) and the most coincident PHA-L and CTB labeled profiles (double-labeling) were selected for electron microscopic observation.

In both single- and double-labeled electron microscopic material, PHA-L immunoreactivity was found exclusively in axonal structures including myelinated and unmyelinated fibers and nerve terminals. While the labeled myelinated and unmyelinated fibers were frequently seen in close apposition to the somata of rubral cells, the majority of labeled nerve terminals were observed in the neuropil. When followed in serial sections, PHA-L labeled unmyelinated fibers sometimes gave rise to boutons en passant (Figure 8A). The labeled terminals were elongated with an average length of 1.7 μ m and width of 0.6 μ m. They were characterized by the presence of numerous centrally located mitochondria and when visible, clusters of pleomorphic synaptic vesicles. The labeled boutons were commonly engaged in symmetric or intermediate synaptic junctions with dendritic shafts of various sizes (Figures 8, 9, 11, 12). From a total of forty-four labeled boutons exhibiting distinct synaptic junctions, 52% synapsed on medium size dendrites (1 > 2 μ m), while 34% contacted small dendrites (\leq 1 μ m). The remaining terminals (14%) were found in synaptic contact with either large dendrites (\geq 2 μ m) or somata.

The ultrastructural appearance of retrogradely transported CTB was described in Chapter 1. In the red nucleus, the electron dense reaction product was found in the somata of small, medium, large, and giant cells (Figures 10, 11, 12) as well as in dendrites larger

than one micron. However, in smaller dendrites the label was difficult to detect and often equivocal. Consistent with the light microscopic observations, the PHA-L labeled myelinated and unmyelinated fibers were seen in direct apposition to the CTB labeled somata of various sizes (Figure 10). However, the PHA-L labeled nigral terminals were never seen in synaptic contact with labeled somata or proximal dendrites. Similar to the observations obtained from the single-labeled material, the PHA-L labeled varicosities overlaying the retrogradely labeled rubrospinal neurons were seen to establish synaptic contact with nearby unlabeled dendrites (Figures 11, 12).

Figure 8: Electron micrographs of PHA-L labeled terminals in single-labeling case #12.

- A: A labeled bouton (B) is engaged in a symmetrical synapse (arrow) with a dendrite (D). The terminal bouton originates from an unmyelinated fiber (arrowheads) and when followed in serial sections was found to be a bouton en passant. Scale bar: $1 \mu m$.
- B: A PHA-L labeled bouton exhibiting pleomorphic synaptic vesicles (open arrow), several mitochondria (M), and multiple synaptic contacts (arrows) with a dendrite (D). Scale bar: $1 \mu m$.

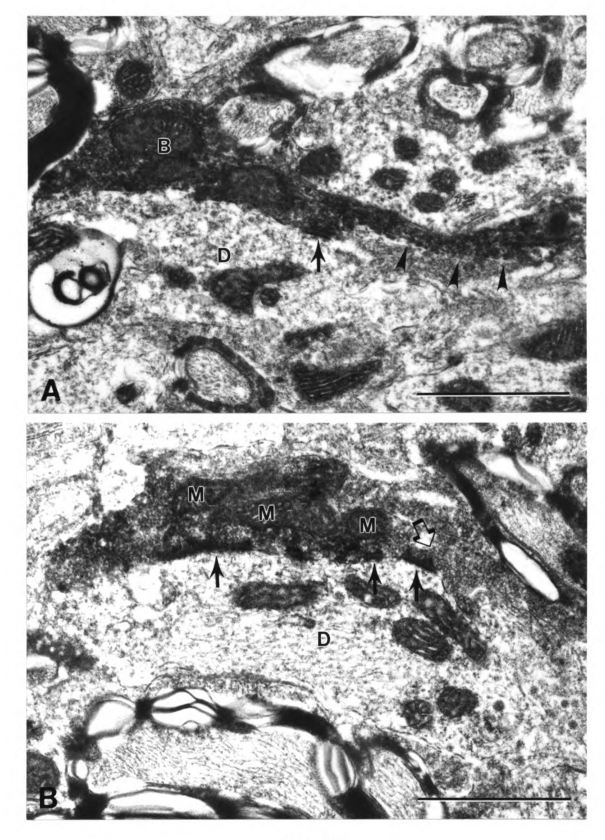


Figure 8

Figure 9: Electron micrograph of single-labeled material showing the relationship of a nigral terminal to a rubral neuron.

A PHA-L labeled bouton synapsing (arrow) on a medium size dendrite (D). The nigral bouton is in close proximity to a large rubral cell body (CB). Scale bar: $1 \mu m$.

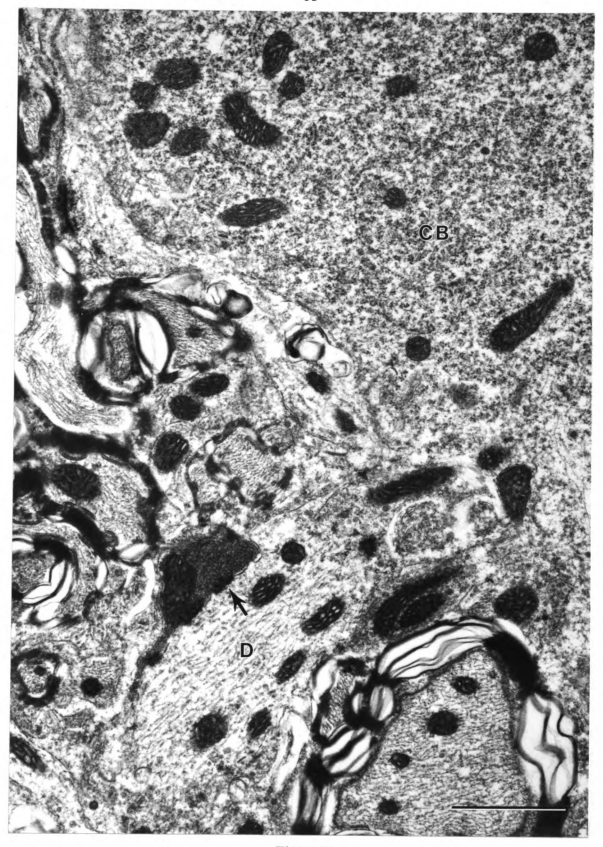


Figure 9

Figure 10: Low power electron micrograph of the double-labeled material.

PHA-L labeled unmyelinated fibers (arrows) apposing the soma of a medium size CTB lableld rubrospinal neuron. The dense reaction product associated with the Golgi complex (arrowheads) makes the labeled cell body easily distinguishable from the unlabeled rubral cell in the upper left corner. Scale bar: $5 \mu m$.

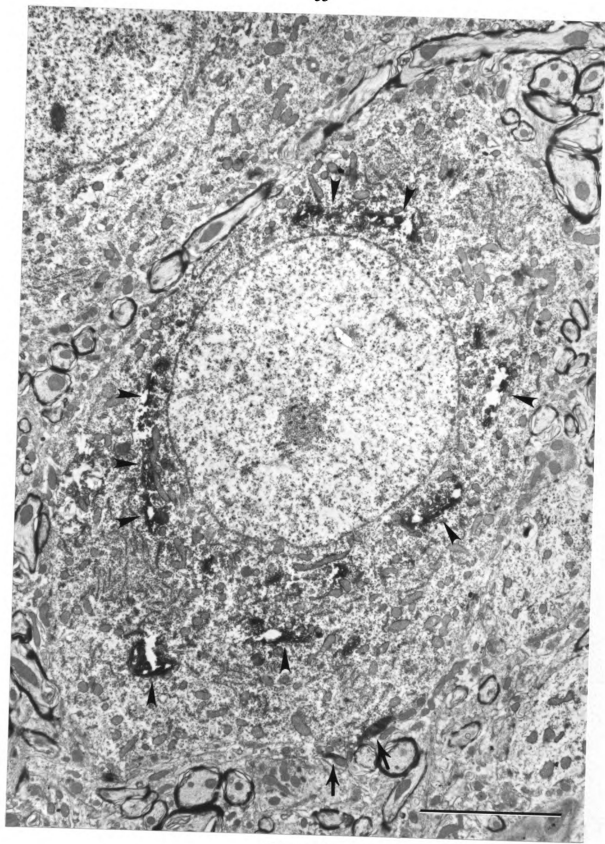


Figure 10

- Figure 11: Electron micrographs illustrating the relationship between a PHA-L labeled nerve terminal and a small CTB labeled cell body in the central portion of the red nucleus.
 - A: Low power micrograph shows a small labeled cell body and a lightly labeled bouton sandwiched between the primary dendrite of the labeled cell and two cross-sectioned dendritic profiles. Scale bar: $5 \mu m$.
 - B: High power micrograph from a serial section of the area outlined in (A). The PHA-L labeled bouton (B) exhibiting numerous pleomorphic vesicles is engaged in synaptic contacts (arrows) with the two small unlabeled dendrites (D1, D2). Note that the nigral terminal is separated from the proximal dendrite of the rubrospinal neuron by a distinct glial membrane. Scale bar: 1 μm.

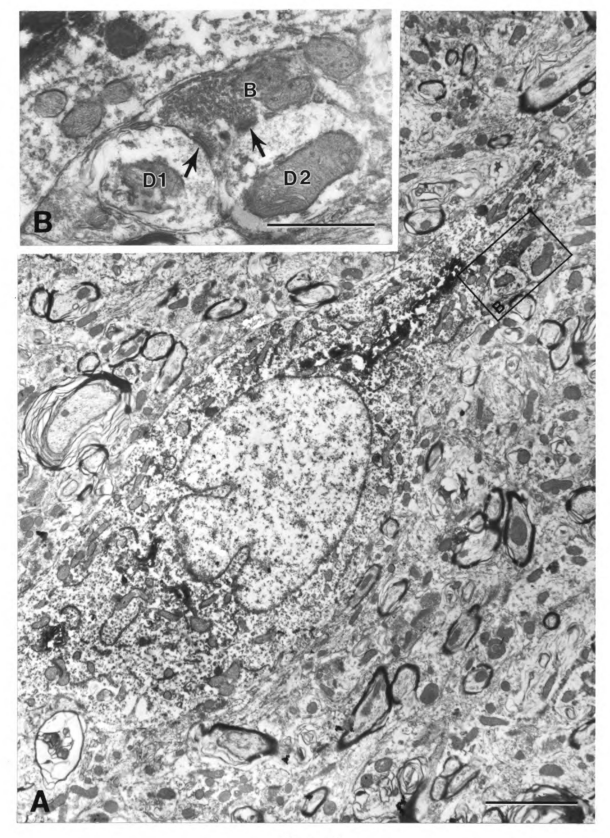
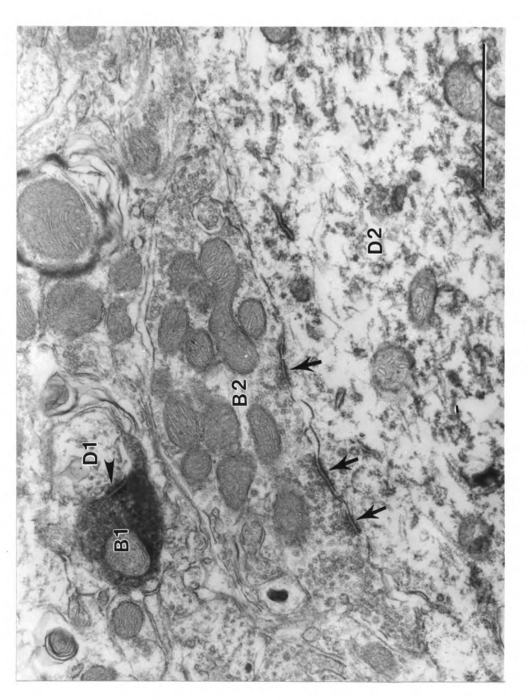


Figure 11

Figure 12: Electron micrograph showing a PHA-L labeled bouton in the neuropil adjacent to a large CTB labeled dendrite.

The PHA-L labeled nigral bouton (B1 is in synaptic contact (arrowhead) with a small unlabeled dendrite while the large labeled dendrite (D2) of a rubrospinal neuron is contacted by a unlabeled bouton (B2). The unlabeled bouton is large, contains round synaptic vesicles, numerous mitochondria, and establishes multiple asymmetric synapses junctions (arrows). Scale bar: $1 \mu m$.



ignre 12

DISCUSSION

The results of the present study demonstrate a new connection which links the SNR to the red nucleus. The nigrorubral fibers distribute to both subdivisions of the red nucleus and terminate almost exclusively on dendrites. Furthermore, the use of a double-labeling method combining anterograde tracing with PHA-L and retrograde labeling with CTB at the electron microscopic level revealed that the nigral terminals do not contact the cell bodies or proximal dendrites of rubrospinal neurons.

Technical considerations. A detailed description of the technical advantages and limitations of the PHA-L and CTB tracing techniques as well as of the double-labeling method employed can be found in Chapter 1. However, it is necessary to further address some technical aspects relevant to this study.

With regard to the demonstration of the nigrorubral connection, one of the major concerns was to exclude the possibility that the PHA-L had labeled rubral afferents which originated from other sources and passed through the substantia nigra. Although the uptake and transport of PHA-L via damaged or intact fibers of passage has been occasionally reported (Cliffer and Giesler, 1988; Schofield, 1989), in our material we have never observed PHA-L transport in this manner. In the context of our experiments, it may be argued that the PHA-L had actually labeled corticorubral fibers passing through the cerebral peduncle and the substantia nigra. In the rat, the corticorubral fibers have been described as fine

strands which exit the cerebral peduncle laterally, and travel through the substantia nigra and medial lemniscus to enter the red nucleus at its lateral border (Brown, 1974). In the present material, the labeled fibers exited throughout the mediolateral extent of the SN and entered both the ventral as well as rostral aspects of the red nucleus. Furthermore, corticorubral fibers terminate almost exclusively in the lateral one-half and rostral one-third of the red nucleus (Brown, 1974; Gwyn and Flumerfelt, 1974), while we have observed a concentration of labeled terminal ramifications in the medial two-thirds of the entire rostrocaudal extent of the red nucleus. Finally, electron microscopic examination of the corticorubral projection has demonstrated that the cortical terminals contain round synaptic vesicles and are engaged in asymmetric synaptic junctions with distal dendrites of rubral cells (Brown, 1974), whereas the PHA-L labeled terminals encountered in our material contained pleomorphic synaptic vesicles and established symmetric synapses predominantly with medium size dendrites. In conclusion, the course, distribution, and mode of termination of the corticorubral projection appears distinctly different from the nigrorubral projection described in the present study.

Technical limitations inherent to the CTB might lead to misinterpretation of the data obtained from the double-labeling experiments. In particular, the fact that the CTB can be taken up by fibers of passage and transported in both anterograde and retrograde directions, and the failure of the tracer to label thin dendrites must be considered. The anterograde transport of CTB from the spinal cord was present in all experiments and was most prominent when the injection involved the white matter and caused considerable mechanical damage. The spinothalamic and spinocerebellar tracts were always to some extent labeled and the brainstem reticular formation consistently contained some labeled fibers. In the light microscopic preparations, the CTB labeled and PHA-L labeled fibers and varicosities can be easily differentiated due to their contrasting colors. However, in the electron

microscopic material the CTB labeled and PHA-L labeled terminals cannot be reliably distinguished from each other since both contain DAB reaction product. While this may pose a serious problem in regions containing congruent anterograde labels, it does not need to be considered with regard to the red nucleus which is not known to receive direct afferents from the spinal cord. In addition, we have never seen anterogradely CTB labeled fibers in the red nucleus in our light microscopic material.

The uptake of CTB by damaged and possibly also undamaged axons has been utilized to its advantage in the present experiments. The rubrospinal tract is known to be somatotopically organized (Shieh et. al., 1983). Neurons projecting to the cervical cord occupy the dorsomedial regions of the red nucleus, while those projecting to the lumbar cord are located in the ventrolateral portion. Therefore, CTB uptake limited to the gray matter of the cervical cord would result in partial labeling of the rubrospinal neurons, and thus might account for our failure to observe synaptic contacts between nigral terminals and rubrospinal neurons. However, since the white matter was invariably involved in the CTB injections, we have always seen labeled neurons throughout the entire nucleus. In particular, in case #31, which was thoroughly analyzed electron microscopically, numerous rubrospinal neurons of different sizes were present throughout the nucleus (Figure 7A). It is therefore unlikely that our failure to detect synaptic contacts between nigrorubral boutons and rubrospinal neurons was due to partial retrograde labeling.

Finally, incomplete labeling of the dendritic trees of the rubrospinal neurons has to be considered. In our electron microscopic material, large and medium size dendrites exhibited distinct electron dense reaction product. However, dendrites thinner than one micron in diameter did not show unequivocal labeling. Although the majority of PHA-L labeled nigral terminals were seen in synaptic contact with unlabeled dendrites thicker than one micron, a few were found synapsing on small dendrites. Therefore, the possibility

remains that a sparse number of nigral boutons may impinge on the distal dendrites of rubrospinal cells.

Organization of the nigrorubral projection. Although the nigrorubral connection has never been described in the rat, it has been documented in degeneration studies using the Nauta-Gygax silver technique in the cat (Afifi and Kaelber, 1965) and monkey (Carpenter and McMasters, 1964). However, electrolytic lesions used in these early experiments inevitably damaged cortical fibers passing in the cerebral peduncle and piercing the substantia nigra on their way to the tegmentum and tectum of the midbrain. Indeed, later studies in the cat (Afifi et. al., 1970) as well as re-examination of the efferent projection of the substantia nigra in the monkey with autoradiographic techniques (Carpenter et. al., 1976) did not substantiate the existence of the nigrorubral projection. In the rat, both the autoradiographic technique (Beckstead et. al., 1979) as well as anterograde tracing with HRP-WGA (Gerfen et al., 1982) failed to demonstrate the nigrorubral connection. This is presumably due to the fact that some nigral fibers pass through the red nucleus on the way to the periaqueductal gray and tectum, and neither the autoradiographic or the HRP tracing techniques could unequivocally differentiate between fibers passing through and terminating within the given area.

In the present study, we have employed the PHA-L tracing method which is extremely sensitive and in contrast to the autoradiographic and HRP techniques, provides solid labeling of axons including thin terminal ramifications and varicosities. This approach allowed us to demonstrate the nigrorubral projection at both light and electron microscopic levels. Although much less prominent than the nigrothalamic, nigrotectal, or nigropedunculopontine projections, the nigrorubral fibers were consistently present in all experiments involving injections in the ventral portion of the SNR. Only when PHA-L

injections were limited to the dorsomedial portion of the SNR was the red nucleus de void of labeled fibers. The nigrorubral projection was strictly ipsilateral and distributed throughout the rostrocaudal extent of the medial two-thirds of the red nucleus. The terminal plexuses were often present in patches which were slightly more prominent in the parvocellular portion of the nucleus. Although the nigral fibers surrounded rubral cells of all sizes, they terminated almost exclusively on dendrites by way of terminals which are morphologically quite similar to the boutons of nigral origin observed in the superior colliculus (Vincent et. al., 1978; Williams and Faull, 1988), motor thalamus (Grofova, 1989), and pedunculopontine tegmental nucleus (Spann and Grofova, 1991). The present double-labeling experiments were inconclusive as to the target neurons of the nigrorubral projection. However, in the light of the electron microscopic observations from the double-labeling experiments, the termination of nigral fibers on rubrospinal neurons appears unlikely.

Functional considerations. The central control of movements is mediated through descending supraspinal tracts originating in the cerebral cortex and brainstem. The activity of the descending pathways is influenced by higher centers which include the cerebellar and basal ganglia systems. While the cerebellum is known to have substantial direct connections with the brainstem, the basal ganglia are thought to control motor functions through the pallido-thalamo-cortical and nigro-thalamo-cortical circuits. However, substantia nigra is known to project to various brainstem nuclei such as optic tectum (Chevalier and Deniau, 1990; Deniau and Chevaleir, 1984; Williams and Faull, 1988) and the medullary reticular formation (Chronister et. al., 1988; Leigh et. al., 1985; van Krosigk and Smith, 1990) which are involved in the control of head and neck movements and orofacial movements (Chandler et. al., 1990), respectively. Therefore, when we discovered the nigrorubral connection we hypothesized that this projection may be involved in the control of rubrospinal neurons

which are known to have an excitatory effect on motorneurons innervating flexor muscles. The existence of this connection would strengthen the evidence that the basal ganglia may directly influence motor functions through monosynaptic pathways involving descending brainstem neurons. Our results suggest that this is not the case, at least not concerning the rubrospinal pathway. Though the possibility still exists that some nigral terminals are in synaptic contact with distal dendrites of rubrospinal neurons, this would represent only a minute population of the nigral boutons found in the red nucleus. Thus, it remains unclear whether the nigral fibers terminate preferentially on a specific sub-population of rubral projection neurons other than the rubrospinal neurons, or whether they are distributed at random and modulate the responsiveness of rubral neurons to other inputs, particularly that from the cerebellum.

BIBLIOGRAPHY

- Afifi, A. and W.W. Kaelber. 1965. Efferent connections of the substantia nigra in the cat. Exptl. Neurol. 11:474-482.
- Afifi, A.D., N.G. Bahuth, and W.A. Maffurij. 1970. Neural connectivity of the substantia nigra. Proceedings of the Ninth International Congress of Anatomy. 4.
- Angaut, P. and F. Cicirata. 1988. The dentatorubral projection in the rat: An autoradiographic study. Behav. Brain Res. 28:71-73.
- Beckstead, R.M., V.B. Domesick, and W.J.H. Nauta. 1979. Efferent connections of the substantia nigra and ventral tegmental area in the rat. Brain Res. 175:191-217.
- Brown, L.T. 1974. Corticorubral projections in the rat. J. Comp. Neurol. 154:149-167.
- Carpenter, M.B. and R.E. McMasters. 1964. Lesions of the substantia nigra in the Rhesus monkey. Efferent fiber degeneration and behavioral observations. Am. J. Anat. 114:293-320.
- Carpenter, M.B., K. Nakano, and R. Kim. 1976. Nigrothalamic projections in the monkey demonstrated by autoradiographic techniques. J. Comp. Neurol. 165:401-416.
- Caughell, K.A. and B.A. Flumerfelt. 1977. The organization of the cerebellorubral projection: an experimental study in the rat. J. Comp. Neurol. 176:295-306.
- Chandler, S.H., J. Turman, Jr., L. Salem, and L.J. Goldberg. 1990. The effects of nanoliter ejections of lidocaine into the pontomedullary reticular formation on cortically induced rhythmical jaw movements in the guinea pig. Brain Research 526:54-64.
- Chevalier, G. and J.M. Deniau. 1990. Disinhibition as a basic process in the expression of striatal functions. TINS. 13:277-280.
- Chronister, R.B., J.S. Walding, L.D. Aldes, and L.A. Marco. 1988. Interconnections between substantia nigra reticulata and medullary reticular formation. Brain Res. Bull. 21:313-317.
- Cliffer, K.S. and G.J. Giesler, Jr. 1988. PHA-L can be transported anterogradely through fibers of passage. Brain Research 458:185-191.

- Daniel, H., P. Angaut, C. Batini, and J.M. Billard. 1988. Topographic organization of the interpositorubral connections in the rat. A WGA-HRP study. Behav. Brain Res. 28:69-70.
- Dekker, J.J. 1981. Anatomical evidence for direct fiber projections from the cerebellar nucleus interpositus to rubrospinal neurons. A quantitative EM study in the rat combining anterograde and retrograde intra-axonal tracing methods. Brain Res. 205:229-244.
- Deniau, J.M. and G. Chevalier. 1984. Synaptic organization of the basal ganglia: an electroanatomical approach in the rat. In Functions of the basal ganglia. Pitman, London, pp.48-63.
- Deniau, J.M. and G. Chevalier. 1992. The lamellar organization of the rat substantia nigra pars reticulata: Distribution of projection neurons. Neurosci. 46:361-377.
- Flumerfelt, B.A. 1980. An ultrastructural investigation of afferent connections of the red nucleus in the rat. J. Anat. 131:621-633.
- Flumerfelt, B.A. and D.G. Gwyn. 1973. The red nucleus of the rat: its organization and interconnections. J. Anat. 118:374-376.
- Flumerfelt, B.A. and A.W. Hrycyshyn. 1985. Precerebellar nuclei and red nucleus. In G. Paxinos (Ed.), The Rat Nervous System Volume 2, Hindbrain and Spinal Cord, Academic Press, Orlando, pp.244-246.
- Garcia-Rill, E. 1986. The basal ganglia and the locomotor regions. Brain Res. Rev. 11:47-63.
- Gerfen, C.R. and P.E. Sawchenko. 1984. An anterograde neuroanatomical tracing method that shows the detailed morphology of neurons, their axons and terminals: immunohistochemical localization of an axonally transported plant lectin, *Phaseolus vulgaris* leucoagglutinin (PHA-L). Brain Research 290:219-238.
- Gerfen, C.R., W.A. Staines, G.W. Arbuthnott, and H.C. Fibiger. 1982. Crossed connections of the substantia nigra in the rat. J. Comp. Neurol. 207:283-303.
- Grofova, I. 1989. Topographical organization of the nigrothalamic projections in the rat. Soc. Neurosci. Abstr. 15:1101.
- Gwyn, D.G. and B.A. Flumerfelt. 1974. A comparison of the distribution of cortical and cerebellar afferents in the red nucleus of the rat. Brain Research 69:130-135.
- Hikosaka, O. 1989. Role of basal ganglia in saccades. Rev. Neurol. 145:580-586.
- Hikosaka, O. and R.H. Wurtz. 1983. Visual and oculomotor functions of monkey substantia nigra pars reticulata. III. Memory-contingent visual and saccade responses. J. Neurophysiol. 49:1268-1284.

- Kennedy, P.R. 1990. Corticospinal, rubrospinal and rubro-olivary projections: a unifying hypothesis. TINS. 13:474-479.
- Leigh, N., J. Mitchell, H. Su, S. Gibson, and J. Polak. 1985. Substantia nigra projections to reticular formation in the rat: retrograde and anterograde tracers and immunocytochemical studies. Neurosci. Lett. 22:S543.
- Massion, J. 1967. The mammalian red nucleus. Phys. Reviews 47:383-346.
- Massion, J. 1988. Red nucleus: past and future. Behav. Brain Res. 28:1-8.
- McLean, I.W. and P.K. Nakane. 1974. Periodate-lysine-paraformaldehyde fixative a new fixative for immunoelectron microscopy. J. Histochem. Cytochem. 22:1077-1083.
- Nakamura, Y., H. Tokuno, T. Moriizumi, Y. Kitao, and M Kudo. 1989. Monosynaptic nigral inputs to the pedunculopontine tegmental nucleus neurons which send their axons to the medial reticular formation in the medulla oblongata. An electron microscopic study in the cat. Neurosci. Lett. 103:145-150.
- Parent, A. 1986. Comparative Neurobiology of the Basal Ganglia. R.G. Northcutt (Ed.), Wiley and Sons, New York.
- Paxinos, G. and C. Watson. 1986. The Rat Brain in Stereotaxic Coordinates, 2nd edn., Academic Press, New York.
- Reid, J.M., D.G. Gwyn, and B.A. Flumerfelt. 1975. Cytoarchitectonic and Golgi study of the red nucleus in the rat. J. Comp. Neurol. 162:337-362.
- Schofield, R.P. 1989. Labeling of axons of passage by *Phaseolus vulgaris* leucoagglutinin (PHA-L). Neurosci. Abstr. 15:306.
- Shieh, J.Y., S.K. Leong, W.C. Wong. 1983. Origin of the rubrospinal tract in neonatal, developing, and mature rats. J. Comp. Neurol. 214:79-86.
- Spann, B.M. and I. Grofova. 1991. Nigropedunculopontine projection in the rat: An anterograde tracing study with *Phaseolus vulgaris*-leucoagglutinin (PHA-L). J. Comp. Neurol. 311:375-388.
- Strominger, R.N., J.E. McGiffen, and N.L. Strominger. 1987. Morphometric and experimental studies of the red nucleus in the albino rat. Anat. Rec. 219:420-428.
- Tracey, D.J. 1985. Ascending and descending pathways in the spinal cord. In G. Paxinos (Ed.), The Rat Nervous System Volume 2, Hindbrain and Spinal Cord, Academic Press, Orlando, pp. 320-321.
- Vincent, S.R., T. Hattori, and E.G. McGeer. 1978. The nigrotectal projection: A biochemical and ultrastructural characterization. Brain Res. 151:159-164.

- von Krosigk, M. and A.D. Smith. 1990. Descending projections from the substantia nigra and retrorubral field to the medullary and pontomedullary reticular formation. Eur. J. Neurosci. 3:260-273.
- Williams, M.N. and R.L.M. Faull. 1988. The nigrotectal projection and tectospinal neurons in the rat. A light and electron microscopic study demonstrating a monosynaptic nigral input to identified tectospinal neurons. Neurosci. 25:533-562.